Magazine of Concrete Research
Volume 68 Issue 4

Creep and residual properties of cracked macro-synthetic fibre reinforced concretes
Serna Ros, Martí-Vargas, Bossio and Zerbino

Magazine of Concrete Research, 2016, **68**(4), 197–207
http://dx.doi.org/10.1680/macr.15.00111
Paper 1500111
Received 08/03/2015; revised 13/05/2015; accepted 15/05/2015
Published online ahead of print 02/07/2015

ice
Institution of Civil Engineers
publishing

Creep and residual properties of cracked macro-synthetic fibre reinforced concretes

Pedro Serna Ros
Professor, ICITECH, Institute of Concrete Science and Technology, Universitat Politècnica de València, Valencia, Spain

José R. Martí-Vargas
Professor, ICITECH, Institute of Concrete Science and Technology, Universitat Politècnica de València, Valencia, Spain

María E. Bossio
PhD student, CONICET, National Council of Scientific and Technological Research, Civil Engineering Department, National University of La Plata, Buenos Aires, Argentina

Raul Zerbino
Professor, CONICET, National Council of Scientific and Technological Research. Civil Engineering Department, National University of La Plata, Buenos Aires, Argentina

This study analysed the creep behaviour of five concretes incorporating 0·5% by volume of four macro-synthetic fibres (MSFs) and one steel fibre. After 28 d moist curing, prisms were pre-loaded up to a crack opening of 0·5 mm and held for 90 d in three different environments – ambient laboratory air, seawater at 45°C and air flow at 45°C. Sustained loads were then applied on three specimens from each group while the other prisms remained unloaded. The remaining residual capacity was evaluated by bending tests. It was concluded that the residual capacity of cracked MSF concretes is not affected by long-term loading.

Notation

f_L	first-peak flexural strength
f_{R1}	residual flexural strength at 0·5 mm
f_{R3}	residual flexural strength at 2·5 mm
w_{cd}	deferred crack opening at the time prior to unloading
w_{ci}	instantaneous crack opening in the loading process during the creep phase
w_{cd}^{j}	deferred crack opening at time j
w_{ci}^{o}	instantaneous crack opening
w_p	maximum crack opening during pre-cracking
w_{pr}	residual crack opening after unloading
φ_w^{oj}	creep coefficient at time j

Introduction

The incorporation of fibres into a concrete matrix controls the cracking processes and thus introduces significant improvements in toughness and durability. Fibre reinforced concrete (FRC) is a high-performance material that is recommended in many applications in order to improve the service life of structures by means of its crack control capacity (Aslani and Nejadi, 2013; Ganesan *et al.*, 2014). When incorporated into concrete, fibres will mainly start to carry stress after micro-cracking of the matrix begins (Mazhar *et al.*, 2013). In the post-cracking stage, the fibres bridge the cracks and control their propagation by means of the chemical and physical bond or anchorage that develops during the fibre pull-out or slip processes (de Montaignac *et al*., 2013).

It has been observed that fibres significantly enhance the static mechanical properties of concrete as well as improving its post-peak response and ductile behaviour (Noushini *et al.*, 2014). The concept of residual stress is now widely accepted as a means of mechanical characterisation of FRC. The residual stress represents the FRC's post-peak capacity for different crack mouth openings. EN 14651 (BSI, 2005) considers four residual stresses for crack opening displacements of 0·5–3·5 mm, and ASTM C1609 (ASTM, 2007) also defines two residual strengths.

Many studies on the behaviour of FRC have been conducted to determine the effects of different types of fibres on the mechanical properties of concrete (Naghibdehi *et al.*, 2014). Most experiences that contributed to the formulation of the FRC chapters in the *fib Model Code for Concrete Structures 2010* (fib, 2013) (MC2010 hereafter) were obtained from concretes reinforced with steel fibres. Although residual stress parameters are applied in structural design, knowledge of the long-term behaviour of FRC in cracked conditions is limited. MC2010 indicates that the long-term performance of FRC could be affected by creep. In general terms, steel fibre filaments do not show creep deformation when subjected to tensile stresses under ambient temperature. MC2010 also mentions that fibre materials with a Young's modulus that is significantly affected by time and/or thermo-hygrometrical phenomena are not covered. In the case of macro-synthetic fibres (MSFs) it is thus of interest to verify the creep behaviour in order to

guarantee their load transfer capacity and ability to control crack widths.

Mackay and Trottier (2004) reported a stable evolution of post-cracking flexural creep of concrete beams reinforced with steel and synthetic fibres statically loaded up to 60% of residual strength over more than a year. Bernard (2010), investigating the magnitude of time-dependent post-crack deflections in shotcrete panels reinforced with steel fibres and MSFs, found that for narrow initial crack widths and load ratios up to 50% of static residual capacity, the steel fibre reinforced shotcrete panels exhibited a stable creep behaviour and, under many circumstances, the macro-synthetic FRC exhibited a higher degree of creep crack widening than steel FRC. However, studying beams loaded up to 50% of their residual capacity at a crack opening of 1·5 mm, Kanstad and Žirgulis (2012) found no differences in the creep behaviour between steel fibres and MSFs, and the residual capacity was not significantly modified by long-term loading.

Previous research on cracked steel FRC (Arango, 2010; Arango *et al*., 2012; García-Taengua *et al*., 2014) found low coefficients of creep at different long-term load levels for a 90 d period, but the type of fibre, the load level and the concrete strength significantly affected the creep behaviour. The authors concluded that the use of fibres, even at low contents, is a good strategy to control flexural creep in the cracked state.

Another study on steel FRC (Zerbino and Barragán, 2012) concluded that stable responses appear for initial crack openings of less than 0·5 mm when applying stresses equal to the stress level at the end of pre-cracking tests and, for crack openings larger than 0·5 mm, sustained stresses lower than 50% of the residual strength corresponding to a crack opening of 3·5 mm were recommended.

The benefits of combining FRC and conventional reinforced concrete in order to reduce deformations and crack widths have also been demonstrated. After 100 cycles of loading, Nakov and Markovski (2012) found that the incorporation of 30 kg/m^3 and 60 kg/m^3 of steel fibres reduced deflections by 16% and 27% and reduced crack widths by 24% and 59% respectively. Similar conclusions were obtained by Vasanelli *et al*. (2013) in a study of macro-synthetic FRC and steel FRC beams submitted to long-term loads in a marine environment; contrary to what occurs in conventional reinforced concrete, the incorporation of fibres led to a stabilisation of crack widths after 10 months under load. Buratti and Mazzotti (2012) showed that although deformability increased, the residual strength capacity was not affected after the application of long-term loads; their results indicate that the steel fibres reduced the deferred strains.

Considering the potential applications of the many new MSFs that are available and the limitations of MC2010, study of the creep behaviour of cracked FRC becomes relevant. This paper presents a study of the creep behaviour of FRC with different types of MSFs in a cracked state. In order to consider the effect of environmental conditions, the cracked specimens were exposed to three different environmental conditions (in ambient air in the laboratory, immersed in seawater at 45°C and exposed to a 45°C air flow) for 90 d.

Materials and method

Experimental programme

Five FRCs incorporating 0·5% by volume of different fibres were prepared – four with MSFs (C1, C2, C3 and C4) and one with hooked-end steel fibres (C5). Twenty four prisms (150 × 150 × 600 mm) and six cylinders (150 × 300 mm) were fabricated from each FRC, and all were cured in a moist room for 28 d.

Age: d		Specimen conservation and testing programme					
1–28		Moist curing: specimens in humidity chamber at 20°C; RH > 95%					
28		All specimens cracked up to 0·5 mm CMOD (24 prisms)					
29–120		Treatment group conditions of cracked specimens					
	Group R (reference) (6 prisms)[a]	Group L (6 prisms) in air in laboratory		Group W (6 prisms) immersed in seawater at 45°C		Group T (6 prisms) exposed to 45°C air flow	
120–210		Specimens conserved in creep chamber at 20°C and 60% RH					
		Group LC Creep loading (3 prisms)	Group LU Unloaded (3 prisms)	Group WC Creep loading (3 prisms)	Group WU Unloaded (3 prisms)	Group TC Creep loading (3 prisms)	Group TU Unloaded (3 prisms)
210		Unloading		Unloading		Unloading	
		Specimens tested in bending up to 4 mm CMOD (18 prisms)					

[a]After unloading, at 28 d, the bending test was completed up to 5 mm CMOD on the group R specimens

Table 1. Experimental programme

The compressive strength was then measured using three cylinders as per standard methods, and the strength and residual stress parameters in bending were obtained on six prisms following EN 14651 (BSI, 2005). In addition, and using the same procedure, the remaining 18 prisms were pre-cracked up to 0·5 mm crack mouth opening displacement (CMOD) and then unloaded. The cracked prisms were classified into three groups of six specimens and exposed to different environmental conditions for 90 d. After this period, they were placed in a dry room (20°C temperature, 60% relative humidity (RH)) where creep tests were performed on three prisms per group while the other three beams remained unloaded. At 210 d after casting, bending tests were performed on all the cracked prisms up to a CMOD of 4 mm in order to evaluate their residual strength capacity. The general scheme of the experimental programme is summarised in Table 1.

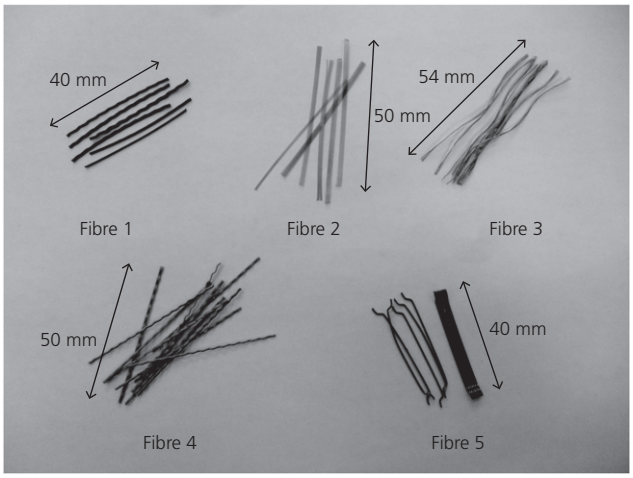

Figure 1. Used fibres

Materials

All the FRCs were prepared by incorporating different fibres to the same base mixture, a self-compacting concrete of 650 mm slump flow. Commercial fibres from different producers were used (see Figure 1 and Table 2). The base mixture was prepared using 290 kg/m^3 CEM I 52·5 type Portland cement, 100 kg/m^3 limestone filler, 900 kg/m^3 crushed sand, 770 kg/m^3 gravel (12 mm maximum size) and an appropriate dosage of modified polycarboxylate-based superplasticiser in order to achieve values of slump flow near the minimum requirements for self-compactability. Table 3 shows the fresh properties and the 28 d compressive strengths of each FRC. As expected, each type of fibre affected the fluidity in a different way.

Exposure environments

Three different environments were selected as follows.

- Laboratory air (group L). In these non-aggressive conditions, only a small amount of matrix–aggregate

	Fibre 1	Fibre 2	Fibre 3	Fibre 4	Fibre 5
Material	Polypropylene	Polypropylene	Polypropylene copolymer	Polypropylene	Steel
Length: mm	40	50	54	50	40
Diameter: mm	0·75	0·62	0·30	0·70	0·62
Slenderness	53	81	158	71	65
Tensile strength: MPa	338	394	570–660	412	1225
Shape	Crimped	—	Torsioned	Crimped	Hooked-end
Elongation: %	15–25%	—	—	15%	—
Elastic modulus: GPa	1·55	4·4	5	—	210
Melting point: °C	150–170	160	325–335	—	—
Fibres per kg	—	73 000	221 000	—	10 000

Table 2. Details of fibres used

FRC	C1	C2	C3	C4	C5
Fibres: kg/m^3	4·5	4·5	4·5	4·5	39
Superplasticiser: kg/m^3	8·6	5·9–8·6	7·3–9·9	7·0–8·6	6·5–8·6
Slump flow diameter: mm	535	495	505	500	540
28 d compressive strength: MPa	42·0	37·1	40·1	42·1	41·4
28 d bending strength, f_L: MPa	3·38	3·45	3·53	3·26	3·80
28 d residual strength, f_{R1}: MPa	1·15	1·76	1·62	0·87	5·14

Table 3. Main characteristics of the studied concretes

interfaces or fibre–matrix micro-cracking due to drying shrinkage could appear.

- Seawater (group W). The prisms were immersed in artificial seawater at 45°C. An isolated vessel with a water heating and recirculation system and proper temperature control sensors was used. Such conditions can affect both the cementitious matrix and the fibres (mainly steel fibres). In accordance with ASTM D1141-98 (ASTM, 2008), 24·72 g/l of NaCl, 0·67 g/l of KCl, 1·36 g/l of $CaCl_2.2H_2O$, 4·66 g/l of $MgCl_2.6H_2O$, 6·29 g/l of $MgSO_4.7H_2O$ and 0·18 g/l of $NaHCO_3$ were used to prepare the artificial seawater.
- Hot air flow (group T). The prisms were placed in an isolated chamber under a 45°C air flow. This condition was selected considering that, in addition to the drying shrinkage effects, hot air can affect the deformability or the bond of the MSFs.

In all cases (L, W and T) the prisms were turned through 90° on the lateral axis to avoid load effects on the current crack.

Creep tests

Creep tests were conducted following the procedure proposed by Arango *et al*. (2012). Creep frames were made from steel profiles to enable loading of three specimens forming a column, guaranteeing test stability over time (Figure 2). Four-point loading over a span of 450 mm was used. The sustained load was adjusted to apply to each prism a nominal stress equal to 70% of the average residual strength at a CMOD of 0·5 mm obtained during the pre-cracking of all the specimens from the corresponding group. A data acquisition system was used to record data from load cells placed in the top of the frames; displacement transducers measured the CMOD for each specimen and temperature and humidity transducers controlled the environmental room conditions. After 90 d, the prisms were unloaded; the measurement and acquisition of CMOD data was continued for 48 h to evaluate the residual deformation.

Creep analysis parameters

Figure 3 shows an idealised stress–crack opening curve for a specimen, including all phases of the testing process (pre-cracking, creep, post-creep unloading and post-creep testing until failure). The parameters considered for analysing the creep behaviour of concrete were as follows.

- Pre-cracking up to a nominal CMOD of 0·5 mm. The following parameters were identified: f_L, first-peak flexural strength (point A); w_p, maximum crack opening; f_{R1}, residual stress at w_p (point B); w_{pr}, residual crack opening after unloading (point C).

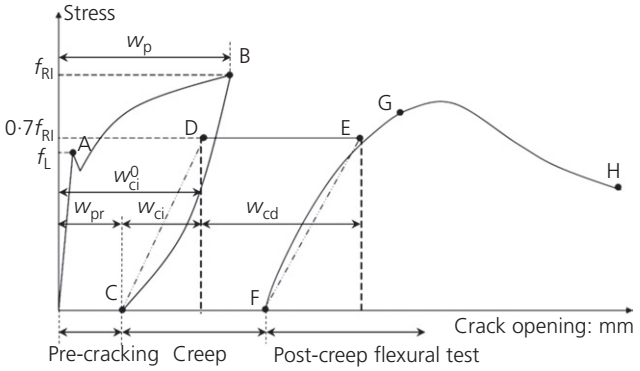

Figure 3. Definition of crack opening parameters for creep test

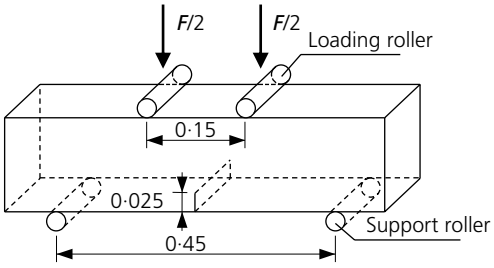

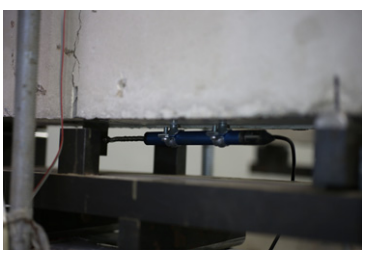

Figure 2. Load configuration and measurement transducers during creep tests (dimensions in m)

		Group L			Group W			Group T		
		Time under loading: d								
FRC		14	30	90	14	30	90	14	30	90
C1	w_{pr}: mm	—	0·30	—	—	0·33	—	—	0·37	—
	Stress: MPa	—	0·73	—	—	0·73	—	—	0·76	—
	w_{ci}: mm	—	0·32	—	—	0·37	—	—	0·39	—
	w_{cd}: mm	0·09	0·17	0·26	0·38	0·43	0·61	0·19	0·25	0·35
	φ_w^{oj}: mm/mm	0·15	0·28	0·42	0·55	0·62	0·88	0·25	0·33	0·46
	CR: 10^{-3} mm/d	6·6	4·9	1·5	27·2	3·3	3·0	13·6	3·6	1·7
	SCR: 10^{-3} mm/d.MPa	9·0	6·8	2·1	37·5	4·5	4·2	17·8	4·7	2·3
C2	w_{pr}: mm	—	0·29	—	—	0·28	—	—	0·28	—
	Stress: MPa	—	1·33	—	—	1·33	—	—	1·28	—
	w_{ci}: mm	—	0·32	—	—	0·43	—	—	0·26	—
	w_{cd}: mm	0·29	0·48	0·63	0·44	0·60	0·87	0·10	0·11	0·14
	φ_w^{oj}: mm/mm	0·47	0·79	1·03	0·61	0·84	1·22	0·18	0·21	0·27
	CR: 10^{-3} mm/d	20·4	12·2	2·4	31·2	10·2	4·5	6·9	1·1	0·5
	SCR: 10^{-3} mm/d.MPa	15·4	9·2	1·8	23·4	7·6	3·4	5·3	0·8	0·4
C3	w_{pr}: mm	—	0·31	—	—	0·30	—	—	0·29	—
	Stress: MPa	—	1·25	—	—	1·25	—	—	1·20	—
	w_{ci}: mm	—	0·36	—	—	0·39	—	—	0·30	—
	w_{cd}: mm	0·20	0·28	0·37	0·56	0·60	0·73	0·15	0·18	0·22
	φ_w^{oj}: mm/mm	0·30	0·42	0·56	0·41	0·87	1·05	0·25	0·31	0·38
	CR: 10^{-3} mm/d	14·0	5·1	1·6	20·3	19·9	2·1	10·4	2·2	0·7
	SCR: 10^{-3} mm/d.MPa	11·2	4·1	1·3	16·3	16·0	1·6	8·7	1·8	0·6
C4	w_{pr}: mm	—	0·35	—	—	0·35	—	—	0·39	—
	Stress: MPa	—	0·61	—	—	0·61	—	—	0·59	—
	w_{ci}: mm	—	0·24	—	—	0·24	—	—	0·12	—
	w_{cd}: mm	0·11	0·17	0·23	0·31	0·36	0·61	0·08	0·10	0·12
	φ_w^{oj}: mm/mm	0·19	0·28	0·39	0·52	0·61	1·04	0·15	0·19	0·24
	CR: 10^{-3} mm/d	7·9	3·6	1·1	21·9	3·1	4·2	5·5	1·3	0·4
	SCR: 10^{-3} mm/d.MPa	13·1	6·0	1·8	36·2	5·1	7·0	9·3	2·2	0·7
C5	w_{pr}: mm	—	0·30	—	—	0·30	—	—	0·32	—
	Stress: MPa	—	3·33	—	—	3·33	—	—	3·28	—
	w_{ci}: mm	—	0·30	—	—	0·20	—	—	0·24	—
	w_{cd}: mm	0·26	0·30	0·35	0·11	0·15	0·18	0·02	0·03	0·04
	φ_w^{oj}: mm/mm	0·44	0·50	0·58	0·21	0·30	0·35	0·04	0·04	0·07
	CR: 10^{-3} mm/d	18·9	2·2	0·8	7·7	2·9	0·4	1·6	0·2	0·2
	SCR: 10^{-3} mm/d.MPa	5·7	0·7	0·2	2·3	0·9	0·1	0·5	0·1	0·1

Table 4. Creep tests results

- Creep test – a sustained stress level of $0{\cdot}7f_{R1}$ was adopted. The parameters considered were: w_{ci}, instantaneous crack opening in the loading process (point D); w_{cd}^{j}, deferred crack opening at time j; w_{cd}, deferred crack opening at the time previous to unloading (point E). The creep coefficient at time j (φ_w^{oj}) is defined as deferred/instantaneous crack opening, where the instantaneous crack opening (w_{ci}^{o}) is referred to the origin ($w_{ci}^{o} = w_{ci} + w_{pr}$).
- Post-creep flexural test. This process evaluates the residual strength of the specimens by composing the total stress–crack opening curve (points F to H); residual strength parameters for greater CMODs can be calculated.

The strength parameters considered in the creep test can be compared with the values obtained in EN 14651 standard tests. The first crack strength (f_L) and the residual strength

(f_{R1}) are exactly those measured during the pre-cracking process. The residual stress calculated for a CMOD of 1·5 mm is not considered because the prisms suffer significant crack opening during the pre-cracking and the creep process; usually, in the final bending test, they achieve this CMOD during the ascending branch (points F to G). However, this is not the case of residual strengths corresponding to wider CMODs, which can be used to evaluate the residual capacity of the prisms after the creep tests. As the residual stress f_{R3}, calculated for a CMOD of 2·5 mm, is applied in MC2010 for FRC classification, it is the value analysed in this work.

Analysis of results

Table 3 shows the results of concrete compressive strength obtained from the cylinders and the first-crack strengths (f_L) and residual stresses (f_{R1}) from the prisms. These results correspond to the mean values from all the beams tested at 28 d (six complete EN 14651 tests for FRC characterisation and 18 only pre-cracked). It can be seen that all the FRCs had a similar concrete compressive strength, in the range 37·1–42·1 MPa, while the bending strength varied between 3·26 MPa and 3·80 MPa.

The residual capacity depends on the type of fibre used, as expected. The highest values correspond to the steel FRC (C5), which showed hardening type post-peak behaviour. For concretes with MSFs, C2 and C3 showed greater residual strength, whereas C1 and C4 had values of f_{R1} lower than 40% of f_L, which indicates low structural post-peak capacity.

The creep test results are summarised in Table 4. The residual crack opening after unloading (w_{pr}), the applied stress during creep tests, the instantaneous crack opening in the loading process (w_{ci}) and the deferred crack opening (w_{cd}) during the periods 0–14 d, 14–30 d and 30–90 d are listed. Table 4 also shows the creep coefficient (φ_w^{oj}), the creep rate (CR, the ratio between deferred strain and time period) and, as the FRCs were subjected to different stresses, the specific creep rate (SCR, ratio between CR and applied stress).

Figure 4(a) compares the results of CMOD evolution for each FRC, and shows the residual crack opening after pre-cracking (w_{pr}), the instantaneous crack opening at loading (w_{ci}) and the deferred crack openings (w_{cd}) at 14 d, 30 d and 90 d. After pre-cracking, the residual cracks were similar in all

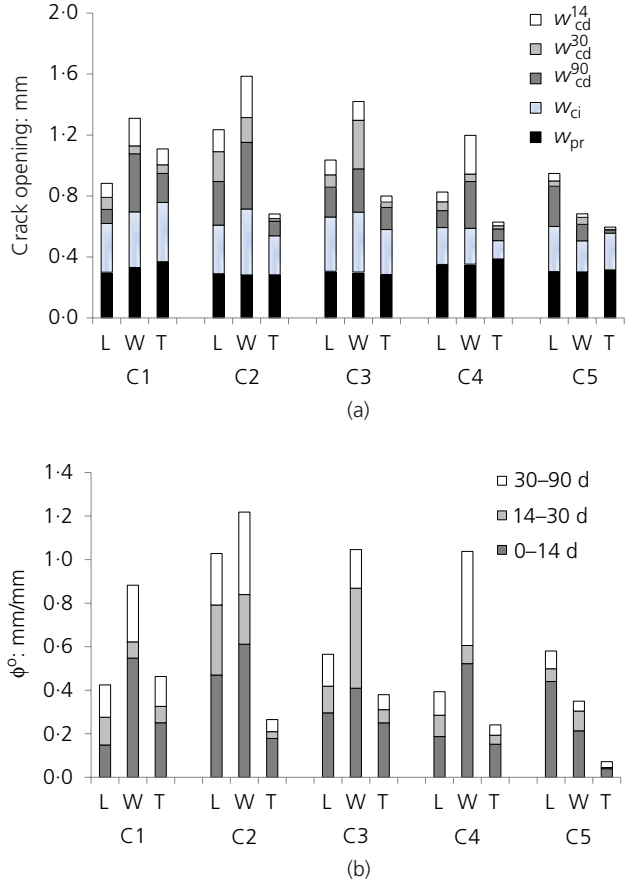

Figure 4. (a) Residual crack opening after unloading (w_{pr}), instantaneous crack opening at loading (w_{ci}) and deferred crack opening after j days (w_{cd}^j). (b) Creep coefficient after 14, 30 and 90 d

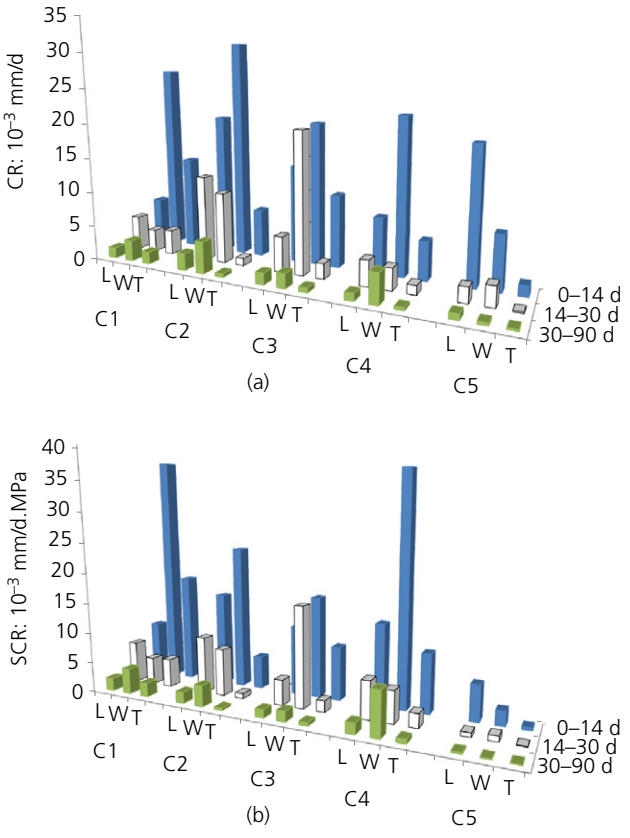

Figure 5. Creep test results: (a) creep rate; (b) specific creep rate

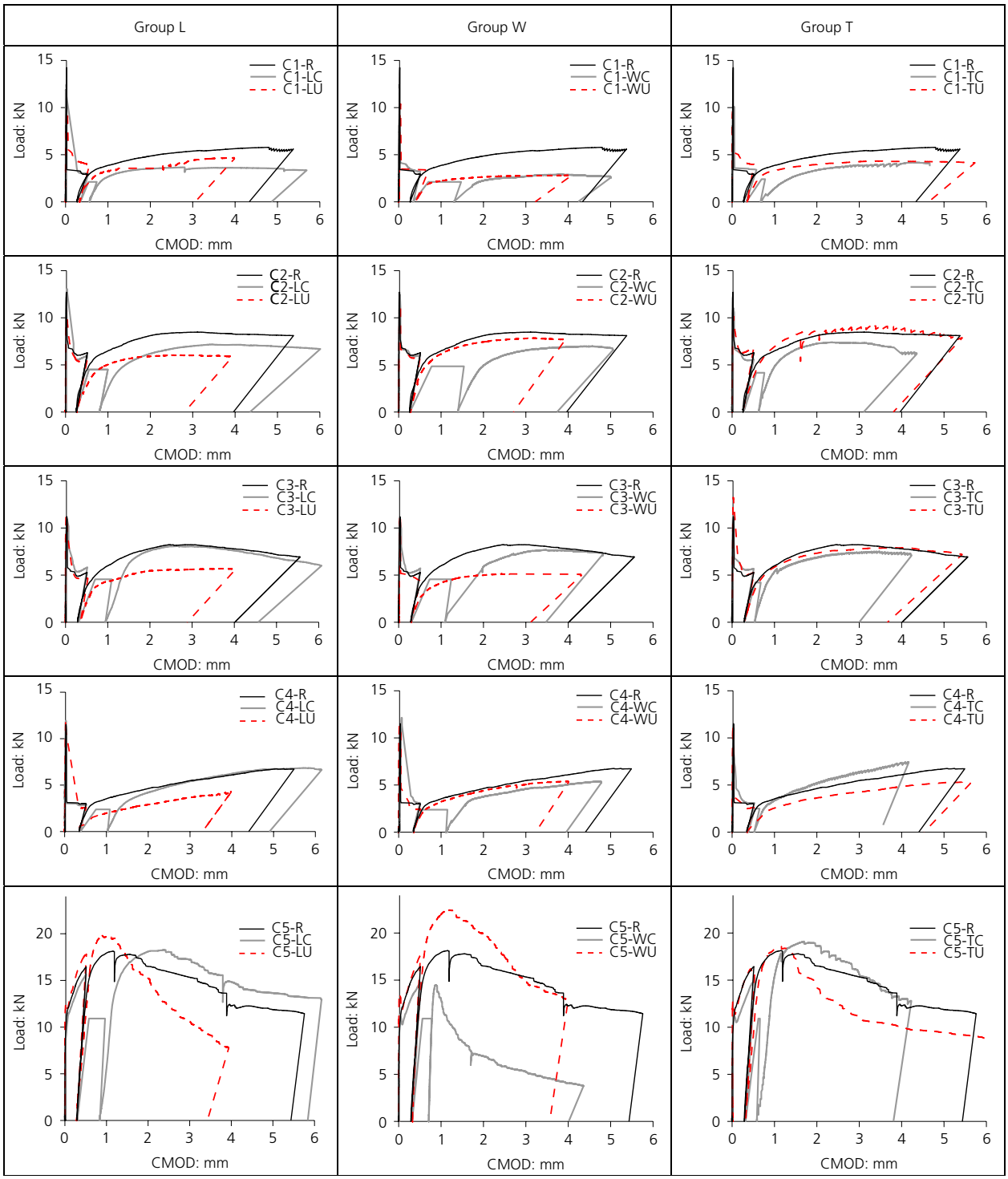

Figure 6. Typical load–CMOD curves

FRCs and close to 0·3 mm. In C2 and C3, the instantaneous crack openings after loading were greater in group W than in groups L or T, which can be associated with some reinforcement degradation; these FRCs also showed higher creep strains. Comparing macro-synthetic and steel fibres, the deferred strains were smaller in C5, and mainly those corresponding to groups W and T. Negative effects in the specimens subjected to hot air flow (group T) were not found – on the contrary, they usually showed lower values of creep. Among the tests on concretes with added MSFs, those corresponding to group W

showed the greater creep values. However, it should be noted that the deferred crack openings were always less than 1 mm.

The creep coefficients of each FRC are compared in Figure 4(b), and the values confirm the observations from Figure 4(a); that is, the group W concretes containing MSFs showed the greater creep values. Figure 4(b) also shows that there is a clear effect from the type of fibre and the environmental conditions. A temperature of 45°C did not have a detrimental effect on the creep behaviour of the tested MSFs; on the contrary, this condition probably enhances matrix strength. Part of the increases in creep strains of the specimens immersed in seawater (group W) can be associated with a drying process together with the long-term load application. The creep coefficients of the steel FRCs (C5) were in most cases smaller than those of the corresponding concretes with MSFs: in the case of group W, the coefficients of C2, C3 and C4 were up to three times higher than those of C5; with the exception of C2, the creep coefficients were similar in group L; for group T, the creep coefficients for all FRCs with MSFs were close and markedly greater than the creep coefficient of steel FRC.

Figures 5(a) and 5(b) compare the values of CR and SCR respectively for different periods of loading (0–14 d, 14–30 d and 30–90 d) for groups L, W and T of the five FRCs. As expected, CR decreased after the first 14 d of loading in all cases (except for a comparison of the 14–30 d and 30–90 d periods for group W of C4). The SCR values showed greater differences between macro-synthetic and steel fibre creep behaviour, being up to 15 times smaller in the latter. C1 and C4 showed higher SCR values than C2 and C3, indicating differences in their residual capacity as discussed later in the paper. In addition, the SCR values in the macro-synthetic FRCs decreased from group W to group L, with the lowest values attained by the group T specimens. The greater creep observed in group W could be associated with loss of water during creep testing.

Figure 6 shows the stress–CMOD curves for each FRC, those corresponding to the six complete bending tests performed at 28 d (group R) and those of the pre-cracked beams; the latter were built from the pre-cracking test plus the creep test (when corresponding) plus the post-creep bending test of the beam that showed intermediate behaviour of each group. It should be noted that no beam failures occurred for the sustained load conditions adopted (near $0{\cdot}7f_{R1}$). It can be seen that there was a significant increase in crack opening in the case of the prisms submitted to long-term loadings, mainly in the case of the macro-synthetic FRCs (C1–C4).

The mean results of the strength and residual capacity of each group are indicated in Table 5 in terms of the first-crack strength (f_L), the residual stresses f_{R1} and f_{R3} and the ratios f_{R1}/f_L and f_{R3}/f_{R1}. It should be noted that when comparing the bending behaviour of the pre-cracked beams with those tested at 28 d, no significant degradation effects on the bending capacity were found for the unloaded specimens or those subjected to long-term loading. There was a small decrease for group W specimens of C1, for both unloaded and loaded specimens. For C5, decreases in residual capacity were not found, with the exception of the loaded specimens of group W where they were significant.

FRC	Group	f_L: MPa	f_{R1}: MPa	f_{R3}: MPa	f_{R1}/f_L	f_{R3}/f_{R1}
C1	R	3·84	1·00	1·65	0·26	1·65
	LU	3·06	1·18	1·09	0·39	0·92
	LC	3·40	1·00	1·08	0·29	1·08
	WU	3·11	1·05	0·89	0·34	0·85
	WC	3·11	1·17	1·05	0·38	0·90
	TU	3·14	1·26	1·40	0·40	1·11
	TC	3·32	1·20	1·28	0·36	1·07
C2	R	3·32	1·79	2·58	0·54	1·44
	LU	3·36	1·53	1·66	0·46	1·08
	LC	3·60	1·81	1·91	0·50	1·06
	WU	3·25	1·59	1·98	0·49	1·25
	WC	3·53	1·82	1·74	0·52	0·96
	TU	3·21	1·72	2·17	0·54	1·26
	TC	3·74	1·91	2·52	0·51	1·32
C3	R	3·21	1·65	2·22	0·51	1·35
	LU	3·60	1·47	1·95	0·41	1·33
	LC	3·32	1·74	2·11	0·52	1·21
	WU	3·55	1·76	2·08	0·50	1·18
	WC	3·80	1·73	1·95	0·46	1·13
	TU	4·01	1·53	2·08	0·38	1·36
	TC	3·61	1·84	2·44	0·51	1·33
C4	R	2·88	0·82	1·27	0·28	1·55
	LU	3·85	1·04	1·48	0·27	1·42
	LC	3·33	0·86	1·40	0·26	1·63
	WU	3·34	0·79	1·30	0·24	1·65
	WC	3·49	0·90	1·13	0·26	1·26
	TU	3·44	0·95	1·43	0·28	1·51
	TC	3·09	0·87	1·50	0·28	1·72
C5	R	3·50	4·72	4·80	1·35	1·02
	LU	3·78	5·54	4·41	1·47	0·80
	LC	3·33	4·77	5·07	1·43	1·06
	WU	4·39	5·79	4·86	1·32	0·84
	WC	3·37	4·65	2·00	1·38	0·43
	TU	3·72	4·89	3·78	1·31	0·77
	TC	4·33	5·09	4·84	1·18	0·95

Table 5. First-peak strength and residual strength parameters

Figure 7 shows the results for f_L and f_{R1}, indicating the original strength of each group, together with f_{R3}, which represents the residual capacity of each group of FRC after exposure to different environmental conditions (R, LU, LC, WU, WC, TU, TC). The figure shows that, with the exception of group W of C5, there were no effects on the residual capacity f_{R3} when loaded and unloaded specimens are compared.

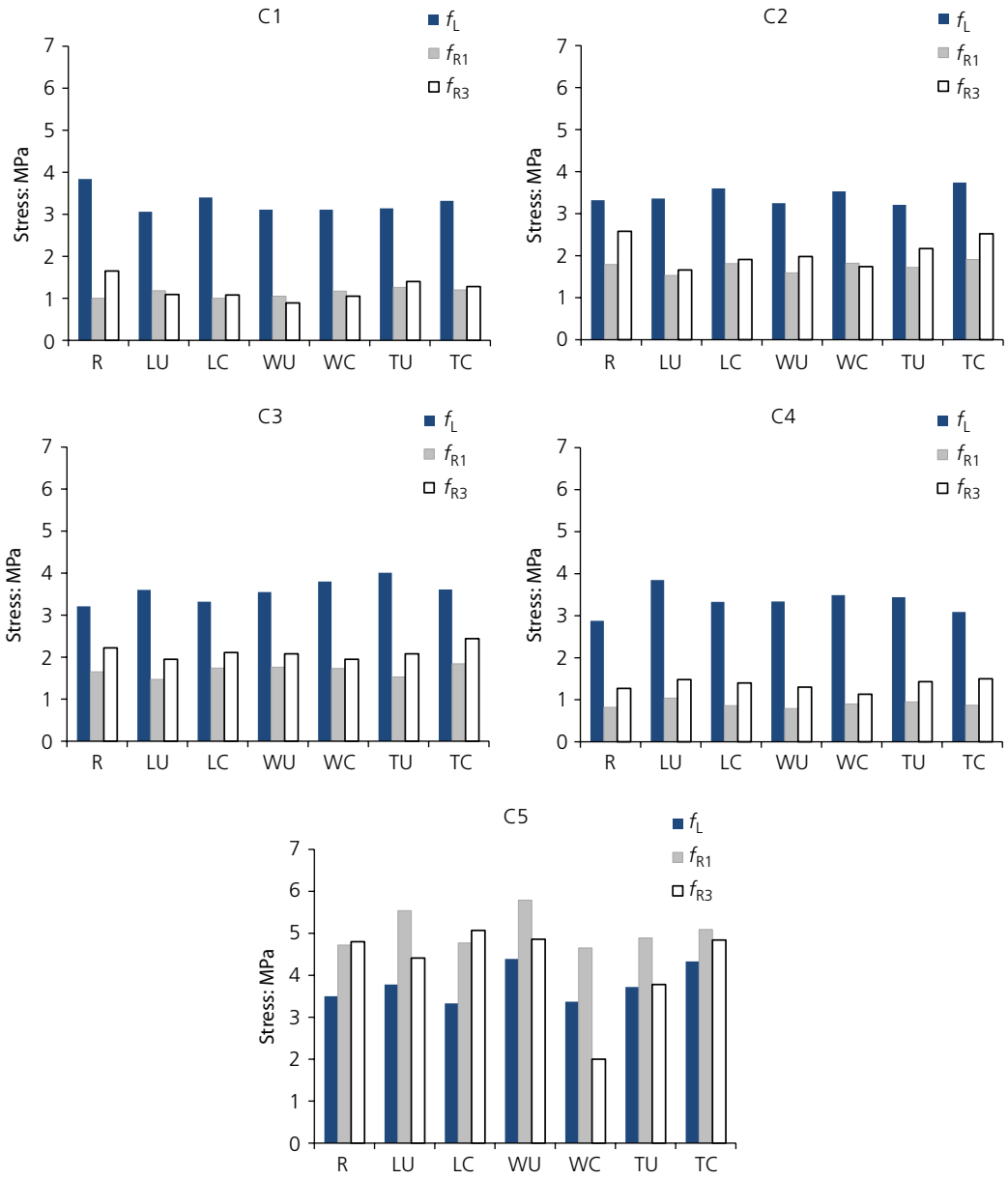

Figure 7. Comparison of first-peak strengths and residual strengths of the different groups

On the contrary, in many cases the residual capacity increased in the prisms subjected to creep. Figures 6 and Figure 7 also show that the residual capacity of the pre-cracked prisms tested at later ages was not modified when compared to the group R specimens, with the exception of group WC of C5. Regarding macro-synthetic FRCs, there was some decrease in residual capacity of C2, an even smaller decrease in C1 in relative terms, and no changes in C3 and C4.

Bearing in mind that the variability of the FRCs themselves may lead to some strength differences between the groups of each FRC, Table 5 includes the results of f_{R1} as relative values of f_L (representing the base concrete bending strength) and the values of f_{R3} relative to f_{R1} (representative of the residual capacity of each prism before exposure to different environmental and loading conditions) in order to analyse the influence of these variables. The results show that the f_{R1}/f_L ratios were similar in the groups of the same FRC, indicating low variability between the different groups of each FRC. Thus, the effects of ageing in different environments and those related to the application of long-term loads can be analysed from the f_{R3}/f_{R1} ratios.

For the laboratory environment, the f_{R3}/f_{R1} ratios of LU and LC groups were similar or slightly smaller, indicating that sustained loading did not affect the residual capacity. For C3, C4 and C5, the LC groups had f_{R3}/f_{R1} ratios similar to those of group R, but were lower in C1 and C2.

For the specimens exposed to hot air flow, there were no great differences between TC and TU, and the ratios were similar to the corresponding L groups (except for C2); there was a reduction in residual capacity when compared with group R for C1, and a minor reduction in C2 and C5.

Regarding the seawater environment, although great differences were not observed, there was a tendency towards lower ratios when group W was compared to group L or group T; the only notable observed degradation was for steel FRC immersed in seawater (C5, group WC).

The experimental work described shows that cracked (0·5 mm) FRC specimens exposed to different environmental conditions and submitted to long-term bending stresses of $0{\cdot}7f_{R1}$ for 90 d do not suffer significant modifications to their residual capacity. Although the incorporation of MSFs resulted in greater CMODs than in the case of steel fibres, the creep rate clearly decreased during the first two weeks and, in any case, behaviour inferring the proximity of beam failure was not observed. After immersion in seawater, the concretes reinforced with MSFs showed better behaviour than steel FRC, as expected.

Conclusions

Creep behaviour in the cracked state and the residual properties of fibre reinforced concrete (FRC) incorporating four different macro-synthetic fibres (MSFs) and one steel fibre were analysed. Before conducting creep tests, cracked specimens were held for 90 d in three different environments – in air in the laboratory (group L), immersed in seawater at 45°C (group W) and exposed to air flow at 45°C (group T). The main conclusions from this study are as follows.

- The type of fibre and environmental conditions can affect creep behaviour and the residual response of FRC. However, with differences found among the studied MSFs and only one type of steel fibre analysed, more tests are necessary to generalise criteria in order to predict the behaviour of a specific FRC.
- Creep strains were greater in concretes reinforced with MSFs than concretes reinforced with steel fibres.
- The crack opening rate significantly decreased after the first two weeks under loading, and no risks of failure were detected for the stress level applied (70% of f_{R1}).
- The crack openings were greatest in group W specimens, followed by those of group L, and lowest in group T specimens.
- The specific creep rate clearly increased in group W specimens of macro-synthetic FRC and decreased by more than an order of magnitude in the steel FRC.
- The residual capacities of cracked macro-synthetic FRCs, even those exposed to seawater, were not significantly affected by long-term loading. On the contrary, there were obvious reductions in the residual capacity of the steel FRC specimens subjected to immersion in seawater.
- For each cracked FRC, the lowest residual capacity usually corresponded to group W and the greatest to group T. Although there were differences in the creep behaviour of the four macro-synthetic FRCs, the differences were smaller than those observed between each environment.
- Comparing the residual capacity after creep tests of groups L, W and T with the residual capacity measured at 28 d (group R), ageing effects were found in macro-synthetic FRC C1, smaller effects in C2, and no changes in C3 and C4. In the same way, no effects were observed in the steel FRC (C5) with the exception of the mentioned reduction in residual capacity observed in the group subjected to seawater treatment (group W).

Acknowledgements

The authors wish to thank the technicians of ICITECH, where the experimental work was developed. The financial support of the project FISNE with reference BIA2012-35776, supported by the Spanish Ministry of Economy and Competiveness and the FEDER fund, is also gratefully acknowledged. The doctoral scholarship of M. E. Bossio was supported by the project EuroTANGO (European Commission – EACEA).

REFERENCES

Arango S (2010) *Flexural Creep of Steel Fibre Reinforced Concrete in Cracked State*. Doctoral Thesis, Universitat Politècnica de València, Valencia, Spain (in Spanish).

Arango S, Serna P, Martí-Vargas JR and García-Taengua E (2012) Test method to characterize flexural creep behaviour of pre-cracked FRC specimens. *Experimental Mechanics* **52(8)**: 1067–1078.

Aslani F and Nejadi S (2013) Mechanical characteristics of self-compacting concrete with and without fibres. *Magazine of Concrete Research* **65(10)**: 608–622, http://dx.doi.org/10.1680/macr.12.00153.

ASTM (2007) C1609/C1609M-12: Standard test method for flexural performance of fiber-reinforced concrete (using beam with third-point loading). ASTM International, West Conshohoken, PA, USA.

ASTM (2008) D1141-98: Standard practice for the preparation of substitute ocean water. ASTM International, West Conshohoken, PA, USA.

Bernard ES (2010) Influence of fiber type on creep deformation of cracked fiber-reinforced shotcrete panels. *ACI Materials Journal* **107(5)**: 474–480.

BSI (2005) EN 14651:2005: Test method for metallic fibered concrete – Measuring the flexural tensile strength (limit of proportionality (LOP), residual). BSI, London, UK.

Buratti N and Mazzotti C (2012) Effects of different types and dosages of fibres on the long–term behaviour of fibre–reinforced self–compacting concrete. In *RILEM PRO88, Proceedings of 8th RILEM International Symposium on Fibre Reinforced Concrete, Guimaraes, Portugal* (Barros J (ed.)). RILEM Publications SARL, Bagneux, France, pp. 177–178.

de Montaignac R, Massicotte B and Charron JP (2013) Finite-element modelling of SFRC members in bending. *Magazine of Concrete Research* **65(19)**: 1133–1146, http://dx.doi.org/10.1680/macr.11.00102.

FIB (Fédération Internationale du Béton) (2013) *fib Model Code for Concrete Structures 2010*. Ernst & Sohn, Berlin, Germany.

Ganesan N, Santhakumar A and Indira PV (2014) Influence of steel fibres on tension stiffening and cracking of reinforced geopolymer concrete. *Magazine of Concrete Research* **66(6)**: 268–276, http://dx.doi.org/10.1680/macr.13.00273.

García-Taengua E, Arango S, Martí-Vargas JR and Serna P (2014) Flexural creep of steel fibre reinforced concrete in the cracked state. *Construction and Building Materials* **65**: 321–329.

Kanstad T and Žirgulis G (2012) Long-time creep testing of pre-cracked fibre reinforced concrete beams. In *RILEM PRO88, Proceedings of 8th RILEM International Symposium on Fibre Reinforced Concrete, Guimaraes, Portugal* (Barros J (ed.)). RILEM Publications SARL, Bagneux, France, pp. 195–196.

Mackay J and Trottier JF (2004) Shotcrete: more engineering developments. *Proceedings of the Second International Conference on Engineering Developments in Shotcrete, October 2004, Cairns, Queensland, Australia* (Bernard ES (ed.)), pp. 183–192.

Mazhar M, Abdouss M, Shariatinia Z and Zargaran M (2013) Grafting of continuous polypropylene fibres by methacrylic acid monomers to improve their bonding to concrete matrix. *Magazine of Concrete Research* **65(13)**: 802–808, http://dx.doi.org/10.1680/macr.13.00010.

Naghibdehi MG, Mastali M, Sharbatdar MK and Naghibdehi MG (2014) Flexural performance of functionally graded RC cross-section with steel and PP fibres. *Magazine of Concrete Research* **66(5)**: 219–233, http://dx.doi.org/10.1680/macr.13.00248.

Nakov D and Markovski G (2012) Time dependant behaviour of SFRC elements under sustained loads. In: *RILEM PRO88, Proceedings of 8th RILEM International Symposium on Fibre Reinforced Concrete, Guimaraes, Portugal* (Barros J (ed.)). RILEM Publications SARL, Bagneux, France, pp. 189–190.

Noushini A, Samali B and Vessalas K (2014) Static mechanical properties of polyvinyl alcohol fibre reinforced concrete (PVA-FRC). *Magazine of Concrete Research* **66(9)**: 465–483, http://dx.doi.org/10.1680/macr.13.00320.

Vasanelli E, Micelli F, Aiello MA and Plizzari G (2013) Long term behavior of FRC flexural beams under sustained load. *Engineering Structures* **56**: 1858–1867.

Zerbino R and Barragán B (2012) Long-term behaviour of cracked steel fibre reinforced concrete beams under sustained loading. *ACI Materials Journal* **109(2)**: 215–224.